SAND2015-2044C

Proceedings of the 34th International Conference on Ocean, Offshore, and Arctic Engineering
OMAE15
May 31–June 5, 2015, St. John's, Newfoundland, Canada

OMAE2015-42288

DRAFT: COER HYDRODYNAMIC MODELING COMPETITION: MODELING THE DYNAMIC RESPONSE OF A FLOATING BODY USING THE WEC-SIM AND FAST SIMULATION TOOLS

Michael Lawson
Braulio Barahona Garzon
Fabian Wendt
Yi-Hsiang Yu
National Renewable Energy Laboratory
Golden, Colorado, USA

Carlos Michelen
Sandia National Laboratories
Albuquerque, New Mexico, USA

ABSTRACT

The Center for Ocean Energy Research (COER) at the University of Maynooth in Ireland organized a hydrodynamic modeling competition in conjunction with OMAE2015. Researchers were challenged to predict the dynamic response of a floating rigid-body device that was experimentally tested in a series of wave-tank tests. Specifically, COER set up a blind competition, where the device specifications and test conditions were released, but the experimental results were kept private until all competition participants submitted their numerical simulation results.

The National Renewable Energy Laboratory and Sandia National Laboratories entered the competition and modeled the experimental device using both the WEC-Sim and FAST numerical modeling tools. This paper describes the numerical methods used to model the device and presents the numerical modeling results. The numerical results are also compared to the experimental results provided by COER at the completion of the competition.

INTRODUCTION

The dynamic behavior of a rigid body floating in an ocean wave field is directly relevant to the design and analysis of many technologies, including surface vessels, underwater vehicles, offshore platforms, and wave-energy converters (WECs). Several numerical methods have been developed to model this type of system, ranging from high-fidelity Navier-Stokes computational fluid dynamics (CFD), which models the relevant fluid-structure interactions from first principles, to mid fidelity time-domain models that assume potential flow, to simple frequency-domain methods.

Floating structures that operate in the ocean wave environment are typically designed with natural frequencies that are outside the range of the most energetic ocean waves they will encounter to minimize hydrodynamic and structural loads. However, the recent emergence of the wave energy industry has seen the deployment of WECs that are designed specifically to have resonance frequencies that match energetic wave frequency to maximize energy extraction.

The Center for Ocean Energy Research (COER) at the University of Maynooth in Ireland has organized a hydrodynamic modeling competition to study the ability of existing numerical tools to model the dynamic behavior of a rigid floating body in a wave field that excites the body's resonance frequencies. COER performed a set of experimental tests on a floating device in both regular and irregular wave fields. The device specifications, all test conditions, and regular wave results were published [1], while the research community was challenged to model the behavior of the device in a specified irregular wave field. Participants in the competition submitted their results to COER without knowing experimental results, and all participants who submitted results were invited to present a paper describing their simulations at a special OMAE2015 session.

This paper describes two submissions to the competition from the National Renewable Energy Laboratory (NREL) and Sandia National Laboratories (SNL). We modeled the device using both the WEC-Sim and FAST numerical modeling tools. WEC-Sim was developed by NREL and SNL specifically to simulate the performance of WEC devices. FAST is a code developed by NREL over the past several decades to model land-based and offshore wind turbines, although it is capable of modeling a wide variety of offshore structures that comprise aerodynamic, hydrodynamic, elastic, and servo components.

This paper describes the WEC-Sim and FAST modeling tools and presents simulation results of the competition device. The next section first provides a brief overview of the floating

device, experimental setup, and competition details. Next, the WEC-Sim and FAST numerical methods and device model setups are described. Finally, we present our numerical results and compare them with experimental results. Note that all numerical results presented in this paper were generated without *a priori* knowledge of the experimental results, which were provided by COER for comparison after simulation results were submitted.

COMPETITION DETAILS

Device Specifications and Experiment Details

All tests were performed at the Kelvin Hydrodynamics Laboratory in the University of Strathclyde, Glasgow, United Kingdom, as described by Costello et al. [1]. The tank used was 2.2 m deep and 76 m long, with a width of 4.5 m. The model was centered in the tank for all experiments.

Figure 1 presents a schematic and illustration of the rigid-body system. The device consists of a submerged cylinder with domed ends and rectangular surface-piercing columns, oriented so its long axis is perpendicular to oncoming waves. The cylinder was connected to a clump mass using inextensible (i.e., inelastic) cables. The motion of the clump mass is restrained to heave using horizontal mooring lines. Costello et al. [1] notes that the cylinder motion was predominantly in the heave and surge directions, whereas pitching motion about the long axis of the cylinder was negligible. Other relevant experimental parameters are presented in

Table 1.

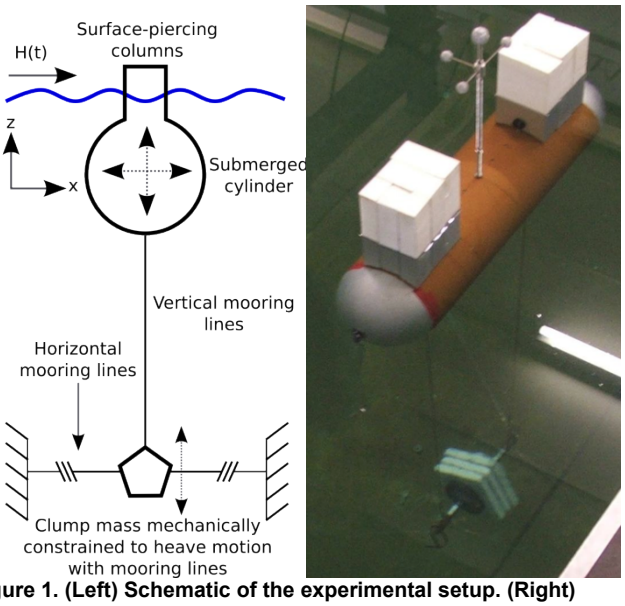

Figure 1. (Left) Schematic of the experimental setup. (Right) Illustration of the experimental device (adapted from [1]).

Table 1. Device specifications (adapted from [1]).

Quantity	Value	Units
Cylinder diameter	0.2	m
Length of cylindrical surface	0.6	m
Length overall	0.8	m
Submergence of centerline	0.2	m
Column X dimension	0.112	m
Column Y dimension	0.15	m
Displacement of cylinder	27	L
Mass of clump mass	19.75	Kg
Length of vert. mooring lines	1.3	m
Tension in vert. mooring lines	176.7	N
Surge stiffness (moorings)	135.9	N/m
Heave stiffness (hydrostatic)	329.6	N/m
Inertia/mass of cylinder	8.9	Kg

Waves

The device was tested in several regular and irregular wave conditions. Regular wave response was measured at wave amplitudes of 12, 25, and 75 mm between wave periods of 0.5 to 4 s. Irregular wave information for the competition was provided in the form of a 512.9-s time-series of wave heights with a measurement frequency of 0.0073 seconds. Wave measurements were made with a wave probe located in the plane of the device so that the wave height was measured at the same time the waves impacted the device. The significant wave amplitude of the competition wave time-series was calculated to be 50 mm by averaging the amplitude of the highest one-third of the waves.

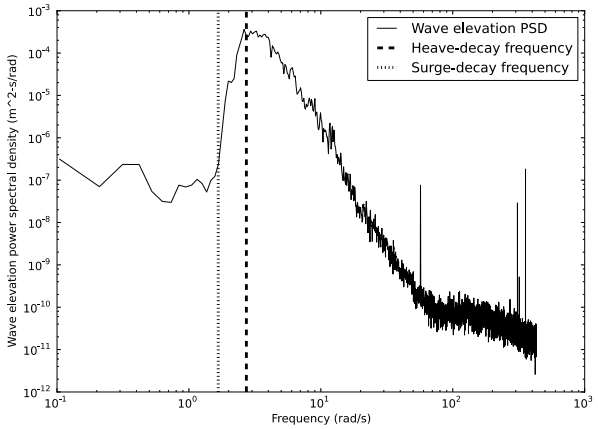

Figure 2. Power spectral density plot of the irregular wave time-series for the competition.

Figure 2 presents a power spectral density (PSD) plot of the competition wave-elevation time-series. The experimentally measured [1] natural decay frequency (referred to interchangeably as the natural frequency in this paper) of the cylinder in surge and heave are also illustrated in Figure 2.

From the PSD, it is clear that the peak period of the waves is about 2.3 s, which is aligned with the heave natural frequency. The surge natural frequency of the rigid body is well below the wave frequencies in the experiment; thus, significant excitation of the surge natural frequency was not expected.

Competition Judging Criteria

COER specified that submissions would be judged based on a comparison of the root-mean-square (RMS) error between simulated and experimental heave and surge motions of the cylinder body. Only the motion experienced during the second half of the time series will be considered so that start-up transients do not affect the results.

Following the submission of the modeling results to COER, the experimental data were released to the competitors to allow comparison between experimental and numerical results. However, contestants were asked not to change their numerical modeling results after submission to allow for a true blind comparison of the various submissions. COER will present the results from all competitors during OMAE2015.

NUMERICAL METHODS

This section describes the numerical methods used by WEC-Sim and FAST and describes the models of the competition device developed using each tool. In addition, both simulations use hydrodynamic coefficients from the potential flow-boundary element method code WAMIT, so a brief description is first presented of the WAMIT simulations that were performed.

Calculating Hydrodynamic Coefficients with WAMIT

WAMIT simulations were performed to calculate the hydrodynamic coefficients of the floating cylinder and surface-piercing columns. A panel mesh, shown in Figure 3, for the simulations was generated using Rhinoceros [2]. WAMIT simulations were performed to calculate the frequency-dependent added mass and radiation damping coefficients for the body. Simulations were performed using first-order waves and the lower-order panel method. Figure 4 presents the hydrodynamic coefficients calculated with WAMIT and compares them to hydrodynamic coefficients for the same body calculated in WAMIT by Costello et al. [1]. A simple grid-refinement study was performed to ensure that mesh resolution did not significantly affect the WAMIT results.

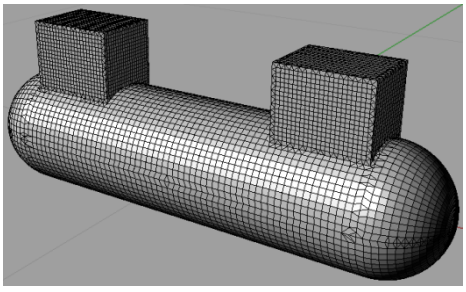

Figure 3. Panel mesh used for WAMIT simulations.

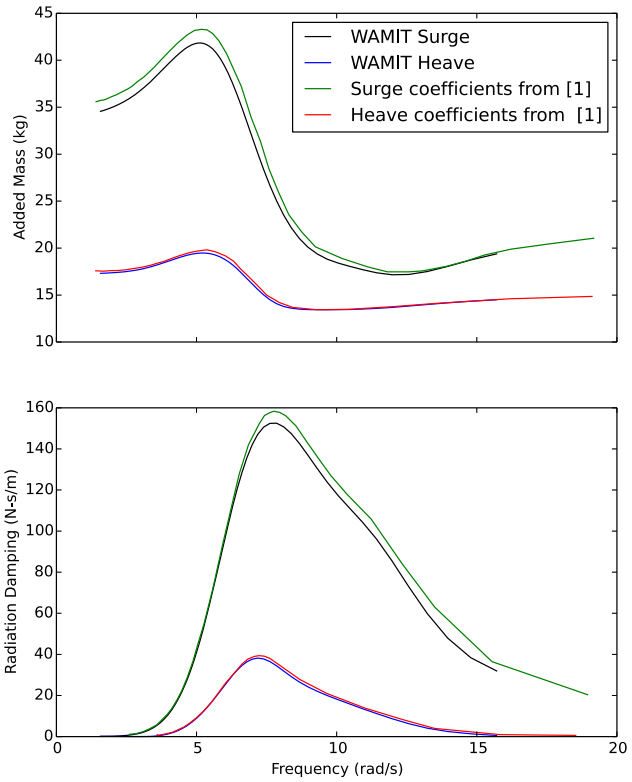

Figure 4. Hydrodynamic coefficients for the floating cylinder and columns.

WEC-Sim

WEC-Sim Model Formulation. WEC-Sim is a simulation tool developed to model the performance of WEC devices in operational wave conditions. The solution method implemented in WEC-Sim closely follows the numerical approach first described by Cummins [3]. At its most basic, WEC-Sim solves the following equation:

$$(m + m_\infty)\ddot{x} = -\int_{-\infty}^{t} f_r(t-\tau)\dot{x}(\tau)d\tau - F_{hs} + F_e + F_{ext} + F_{visc}, \qquad (1)$$

where m and m_∞ are the body mass and infinite frequency-added mass, respectively, and x is position vector. The first term on the right-hand side of Eq. (1) is the convolution integral that models the wave radiation forces. F_{hs}, F_e, F_{ext}, and F_{visc} are the hydrostatic, wave excitation, external forces (e.g., power take-off [PTO] and mooring), and viscous forces, respectively. Hydrodynamic coefficients needed to solve Eq. (1) are typically derived from potential flow-boundary element method codes, such as WAMIT [4] or Nemoh [5].

WEC-Sim is implemented in the MATLAB SimMechanics multibody dynamics environment. WEC models are constructed using custom-developed building blocks and drag-and-drop functionality, as illustrated in the next section. More information on the formulation of the WEC-Sim model and its implementation are available in Refs. [6] and [7].

To improve the capabilities of WEC-Sim, we recently implemented buoyancy and Froude-Krylov forces calculated

from the instantaneous position of the body with respect to the free surface. Although these capabilities were not used in this paper, we plan to explore the effect that these more advanced hydrostatic and hydrodynamic models have on the simulation results in future work.

WEC-Sim Model Setup. The experimental device was modeled in WEC-Sim v1.0 as the two-body system illustrated in Figure 5. The cylinder and surface-piercing columns were represented as a single rigid body numerically constrained to move in the heave and surge directions only. The cylinder body was connected to the clump mass through a massless rigid connection with ball joints on either side. The clump mass was numerically constrained to heave motion only. The ball joints were necessary to allow the cylinder body to move in surge without inducing pitch motion, thus accurately representing the experiment. The vertical mooring stiffness of the clump mass was modeled as a vertical linear spring stiffness, k_{m-h}, provided in Costello el al. [1]. The surge restoring force on the cylinder body was accounted for through the explicit simulation of the connection between the floating body and the clump mass. Figure 6 shows the implementation of this model setup in the WEC-Sim environment.

Linear hydrodynamic coefficients from WAMIT described in the previous section were used to determine the added mass, radiation damping, and wave excitation forces for the cylinder body. Only the surge and heave components (1-1, 3-3, 1-3, and 3-1) of these coefficient matrices were used. The viscous drag coefficient of the cylinder body was modeled as having a linear and a quadratic component. The linear component was calculated from the experimental free-decay tests [1], whereas the quadratic drag component was tuned by matching experimental and numerical response amplitude operator (RAO) plots, as described in the *Results* section of this paper. The volume of the cylinder body and its hydrostatic stiffness were calculated from the geometry provided by COER [8]. The clump mass volume was calculated so that the entire system was neutrally buoyant in the equilibrium position specified by Costello et al. [1]. All other properties of the cylinder body and clump mass are summarized in Table 2.

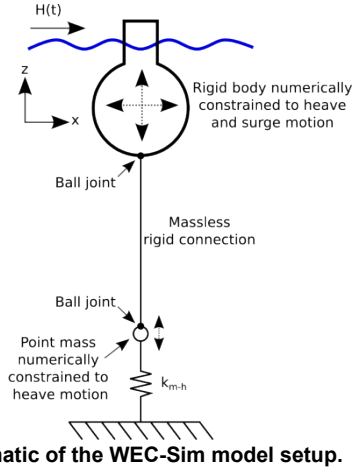

Figure 5. Schematic of the WEC-Sim model setup.

Table 2. Model parameters for the cylinder body and clump mass.

Cylinder	Mass (kg)	8.99
	Volume (m^3)	0.027
	Hydrostatic Stiffness 33 (N/m)	329.6
	Linear Drag 11 (N/(m/s))	1.52818574
	Linear Drag 33 (N/(m/s))	2.49222
	Quadratic Drag 11 ($N/(m^2/s^2)$)	126.75
	Quadratic Drag 33 ($N/(m^2/s^2)$)	25
	Added Mass 11, 33, 13, 31 (kg)	WAMIT
	Radiation Damping 11, 33, 13, 31 (N/(m/s))	WAMIT
	Wave Excitation 11, 33	WAMIT
Clump	Mass (kg)	19.75
	Added Mass (kg)	1.02
	Mooring Stiffness (N/m)	36.3
	Volume (m^3)	0.0017839

The hydrodynamics of the clump mass were greatly simplified. Wave excitation, radiation damping, and viscous drag where neglected because the clump mass was small with respect to the cylinder body and submerged far below the free surface where hydrodynamic forces and wave orbital velocities are small. It follows that the added mass was considered to be frequency independent. All values for mass, added mass, and mooring stiffness used for the present simulations are summarized in Table 2.

Simulations were performed within the time domain using a time step of 0.01. This time step provided a sufficient balance between temporal resolution (approximately 200 time steps peak wave period) and run time. MATLAB's ode4 solution algorithm was used to advance the solution in time. Simulations of the 500-s irregular time series took about 300 s using a standard laptop computer.

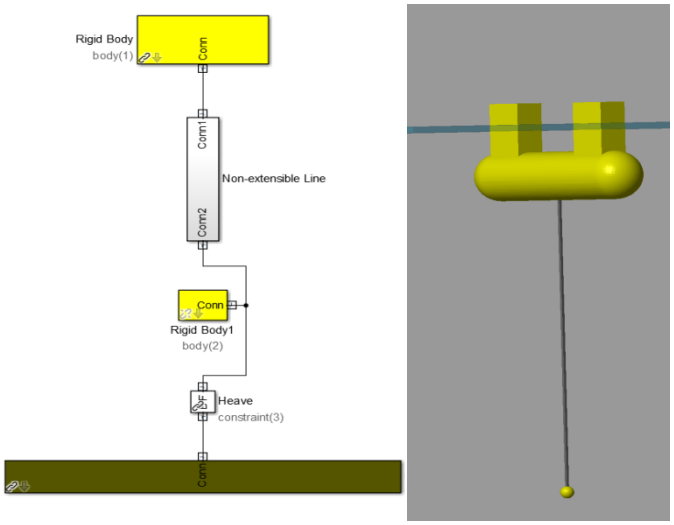

Figure 6. WEC-Sim block diagram system representation. (Left) A block diagram representation of the model. (Right) Model visualization in WEC-Sim.

FAST

FAST is a numerical modeling tool developed by NREL over the past several decades to model the dynamic response of wind turbines. FAST joins aerodynamics models, hydrodynamics models for offshore structures, control and electrical system (servo) dynamics models, and structural (elastic) dynamics models to enable coupled nonlinear aero-hydro-servo-elastic simulation in the time domain (see [9] for more details). Accordingly, although FAST was developed for wind-turbine modeling applications, it has the capability to model arbitrary-geometry floating bodies, such as the COER competition device.

The floating device was modeled with the latest release of FAST (v8.09.00a-bjj) [9]. Three different approaches are available in FAST v8 to model hydrodynamic loads: a strip-theory approach based on Morison's equation, a potential-flow (radiation/diffraction) approach, and a hybrid combination of both methods (radiation/diffraction and the drag component of Morison's equation). Because of the nature of the available device specifications and the fact that the problem did not involve any water currents, we selected a modeling approach based on potential flow. The linear potential-flow approach implemented in FAST v8 considers wave radiation, wave diffraction, and hydrostatic restoring forces through a set of frequency-dependent matrices computed via WAMIT. Second-order drift forces can also be considered in the current version of FAST v8; however, this feature was not used for this specific problem. A detailed review of the linear potential-flow-based hydrodynamics model implemented in FAST is given in [10].

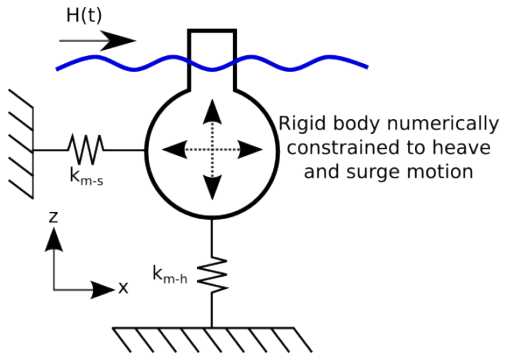

Figure 7. FAST model schematic.

Model Setup. The device was modeled as a single body within the FAST v8 environment, as illustrated schematically in Figure 7. A single-body model setup was selected because the current version of FAST does not have the ability to easily model two floating bodies connected with joints.

To model the two-body system as a single rigid body, the mass and added mass of the clump mass were added to the heave component of the added-mass matrix of the cylinder body. The motion of the rigid body was numerically restricted to heave and surge only. Mooring stiffness in both heave and surge were modeled as linear springs with coefficients provided in Costello et al. [1]. Hydrodynamic drag was modeled using a combination of linear and quadratic drag. The linear drag coefficient was taken from the experimental results [1], whereas the quadratic drag coefficient was tuned using RAO plots as described in the Results section. All other simulation properties were the same as those described in the time-domain model of Costello et al. [1]. Simulations were performed with a time step of 0.0073 s and ran in about 210 s using a standard laptop computer. This time step was selected because it matched the measurement frequency of the experimental data and provided sufficient temporal resolution.

RESULTS AND DISCUSSION

WEC-Sim and FAST were used to perform three sets of simulations:

1. Free-decay simulations
2. Regular-wave simulations
3. Irregular-wave simulations using the competition wave time-series.

This section presents the results from each set of simulations and compares and contrasts the results with the experimental results of Costello et al. [1]. Comparisons of the irregular-wave results were made between 250 and 500 s, unless otherwise specified.

Free-Decay Test Results

Free-decay tests of heave and surge motion were carried out to perform a preliminary verification of the model. Table 3 presents the results of the free-decay simulations and the relative percent error with respect to the experimentally measured results. FAST was shown to be in close agreement with the experimental results (<1% error), whereas WEC-Sim under predicted the decay periods by less than 3%. We did not explore what caused the discrepancy between the WEC-Sim and experimental results because of the compressed time schedule of the competition, so this task is left to future research efforts.

Table 3. Free-decay test results for WEC-Sim and FAST.

	Experimental [1]	WEC-Sim	FAST
Surge free-decay period	3.77	3.67	3.78
% error in surge-decay period	–	-2.6%	0.46%
Heave free-decay period (s)	2.31	2.26	2.30
% error in heave-decay period	–	-2.16%	-0.13%

Regular-Wave Simulations and Estimating Viscous Drag Coefficients

Next, the device was simulated in regular waves with amplitudes of 25 and 75 mm and periods between 1 and 4 s. Figure 8 compares the WEC-Sim and FAST results to frequency-domain simulations and experimental data [1]. The quadratic heave and surge viscous drag coefficients for the 25- and 75-mm simulations were tuned so that the numerical RAOs matched the experimental RAOs. In the surge direction, the quadratic drag coefficient was tuned so that the RAO matched the overall trend of the experimental data. In the heave direction, the quadratic drag coefficient was tuned so the resonance peak at 2.31 s was approximately matched. Table 4 shows the viscous drag coefficients that were selected for WEC-Sim and FAST. Overall, the numerical and experimental RAOs showed good agreement once the quadratic viscous drag coefficients were tuned, providing confidence in the FAST and WEC-Sim models.

As previously discussed, the competition wave time-series has a significant wave amplitude of about 50 mm. Thus, to tune the numerical models for the irregular-wave simulations, we averaged the 25- and 75-mm quadratic viscous damping values. These values are also presented in Table 4.

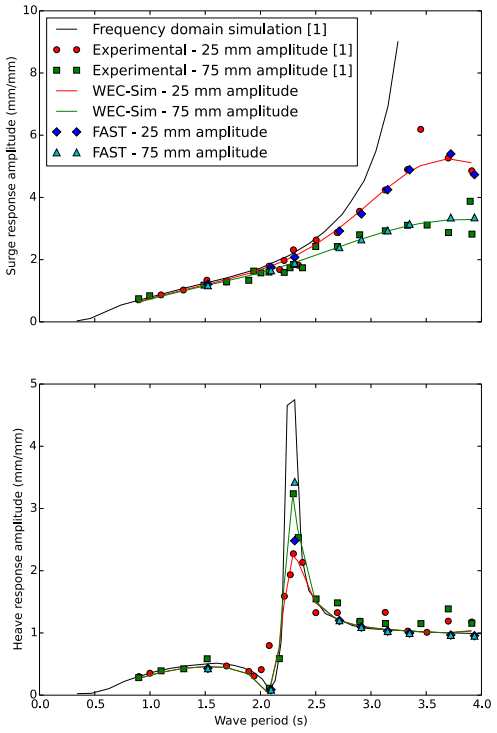

Figure 8. Response amplitude operator plots for surge (top) and heave (bottom). The plots show a comparison of the results from the frequency-domain simulations with no viscous drag [1], experimental data [1], WEC-Sim simulation results, and FAST simulation results.

Table 4. Viscous drag coefficients used for WEC-Sim and FAST simulations determined from RAO tuning.

	WEC-Sim	FAST
25-mm surge quadratic drag coefficient	135.0	93.0
25-mm heave quadratic drag coefficient	28.5	7.8
75-mm surge quadratic drag coefficient	118.5	98.0
75-mm heave quadratic drag coefficient	21.5	16.0
50-mm surge quadratic drag coefficient used for competition wave time-series simulations	126.75	95.5
50-mm heave quadratic drag coefficient used for competition wave time-series simulations	25.0	11.9

Irregular-Wave Simulations

WEC-Sim and FAST were used to simulate the dynamic response of the experimental system in the competition wave time series. The first step in analyzing the numerical results was to compare the wave excitation forces from WEC-Sim and FAST. The two codes use different methods for calculating the excitation forces: WEC-Sim uses a wave-exciting kernel convoluted with the wave time-series, whereas FAST computes the magnitude and phase of the irregular time-series [10]). However, the forces from both codes were found to agree to within 32-bit machine precision.

Next, we compared the numerical and experimental root mean square (RMS) and RMS error values of surge and heave motion between 250 and 500 s, and Table 5 shows the results of this comparison. It is relevant to note that the dominant surge-motion excitation frequencies were not near the surge resonance, whereas the heave excitation frequencies were aligned with the heave-motion resonance, as shown in Figure 2. As such, small errors in damping and discrepancies between the experimental and numerical model setups are expected to cause more error in heave than surge. Accordingly, small discrepancies in the numerical and experimental models may explain some of the differences in the experimental and numerical results. In addition, small phase shifts in the experimental and numerical results will lead to significant RMS errors, even when the qualitative behavior and peaks of the motion are correctly predicted.

Table 5. Comparison of RMS values for experimental results and numerical results from WEC-Sim and FAST.

	Experimental	WEC-Sim	FAST
Surge RMS (m)	0.0397	0.0405	0.0401
RMS surge error (m)	–	0.0142	0.0136
Heave RMS (m)	0.0229	0.0250	0.0275
RMS heave	–	0.0132	0.0121

error (m)			

Although studying average quantities, such as RMS, is useful, directly comparing time series provides additional insight into how the experimental and numerical results compare. Figure 9 and Figure 10 present time-series comparisons of the heave and surge response of the cylinder body across two different time periods. During the time period in Figure 9, both numerical models do a good job predicting the dynamic motions of the body, whereas in the time period in Figure 10, the heave motions are not well predicted. It is not immediately obvious what it is about the wave field in Figure 9 that allows the numerical models to do a better job predicting the heave motion compared to the wave field of Figure 10. From a qualitative perspective, the FAST code appears to more accurately predict heave motions.

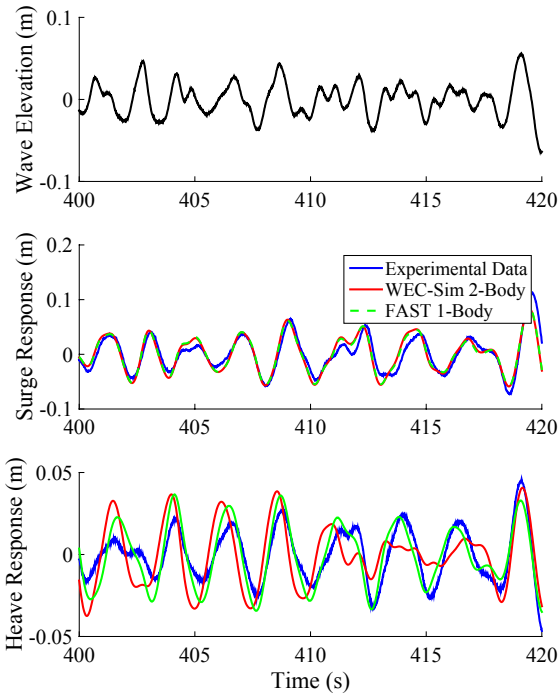

Figure 9. Dynamic response of the cylinder body between 400 and 420 s. During this period of time, there is good qualitative agreement in both the heave and surge response.

To better understand the discrepancies between the numerical and experimental results, we performed a frequency-domain analysis of the surge and heave responses between 250 and 500 s. Figure 11 and Figure 12 present the frequency-domain analysis results in the form of PSD plots of surge and heave motion, respectively. The frequency-domain content is plotted between wave periods of 1 and 10 rad/s (0.63 to 6.3 second period), which is the frequency range within which virtually all the wave-excitation energy is contained. The surge-motion PSD shows excellent agreement between the experimental and numerical frequency content in the regions of highest wave energy. The peak in the surge-motion frequency responses are well aligned and the PSD plots remain well aligned across all frequencies in which there is significant wave excitation.

Conversely, the heave-motion PSD plots show a few small, but possibly significant, discrepancies. Specifically, the peak location and magnitude in the experimental and numerical heave PSD motions are slightly different, with the experimental PSD having a slightly lower frequency. In addition, there is a possible significant discrepancy in the PSD plots between about 3 and 3.75 rad/s (identified with the dashed shape in Figure 12),

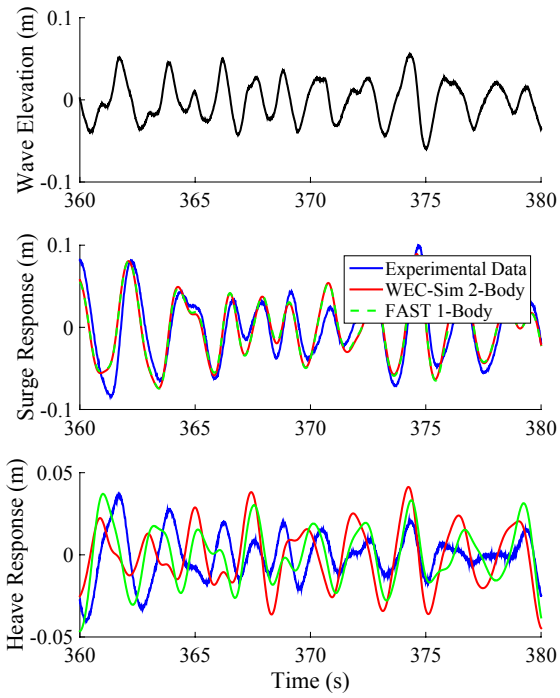

Figure 10. Dynamic response of the cylinder body between 360 and 380 s. During this period of time, there is good qualitative agreement in the surge-motion response, whereas the heave motions are in poor agreement.

but further investigation is needed to determine the cause of this discrepancy. The short timeframe of the COER competition did not allow for this discrepancy to be further studied, therefore it will be covered in future research.

CONCLUSION

The device specified in the COER hydrodynamic modeling competition [8] was simulated using the WEC-Sim and FAST numerical modeling tools. The numerical tools were used to predict the surge- and heave-decay frequencies of the device as well as the device response in regular and irregular wave fields. The numerical results for the irregular-wave simulations, which were obtained without *a priori* knowledge of the experimental results, were compared to the experimental results. Overall, the numerical and experimental data were shown to be in good qualitative and quantitate agreement in surge, whereas the agreement was not as good in heave. The exciting wave field has a peak period that was very close to the natural period of

the device in heave, whereas the natural surge period was significantly below the predominant frequencies of the wave field. Accordingly, it was expected that the heave results comparison would be very sensitive to small discrepancies in the experimental and numerical setups, possibly explaining some of the observed discrepancies in the numerical and experimental results.

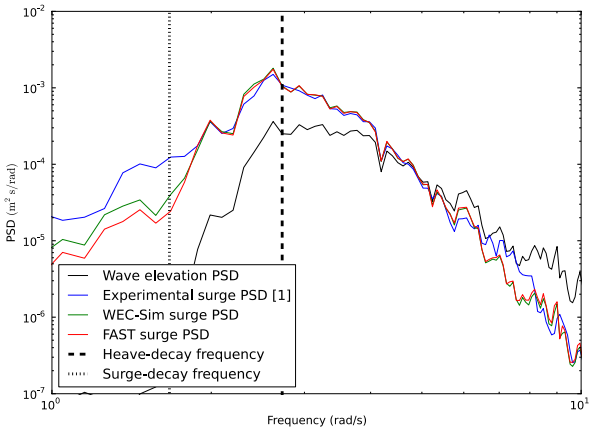

Figure 11. PSD of the surge motion calculated using results between 250 and 500 s. Note that the wave PSD and device natural frequencies are also shown for reference.

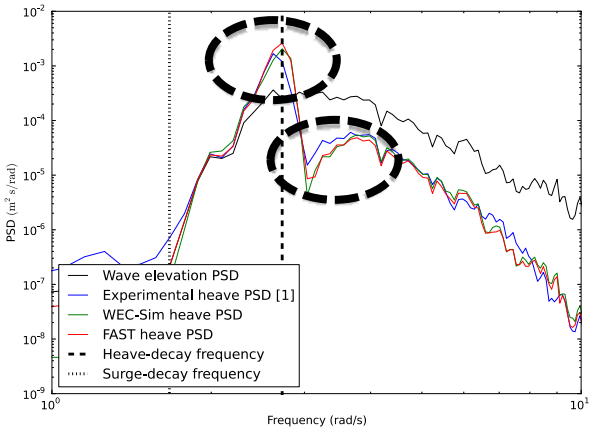

Figure 12. PSD of the heave motion calculated using results between 250 and 500 s. Note that the wave PSD and device natural frequencies are also shown for reference. The dashed lines identify regions where there is significant disagreement in the heave response PSD plots.

The results presented in this paper suggest a direction for future research. Specifically, future work is needed to study the cause of the discrepancies between the results from the two numerical models and between the numerical and experimental results. The authors anticipate that the results from other participants in the competition will also help identify areas for improvement in the WEC-Sim and FAST codes.

ACKNOWLEDGMENTS

The authors would like to thank Andrew Platt and Jason Jonkman for their assistance using the FAST modeling code. Levi Kilcher provided generous assistance performing frequency-domain data analysis. Nathan Tom provided critical help performing the WEC-Sim simulations.

This work was supported by the U.S. Department of Energy under Contract No. DE-AC36-08GO28308 with the National Renewable Energy Laboratory. Funding for the work was provided by the DOE Office of Energy Efficiency and Renewable Energy, Wind and Water Power Technologies Office.

Sandia National Laboratories is a multiprogram laboratory managed and operated by Sandia Corporation, a wholly-owned subsidiary of Lockheed Martin Corporation, for the U.S. Department of Energy's National Nuclear Security Administration under contract DE-AC04-94AL85000.

REFERENCES

[1] R. Costello, J. Davidson, D. Padeletti, and J.V. Ringwood, "Comparison of Numerical Simulations with Experimental Measurements for the Response of a Modified Submerged Horizontal Cylinder Moored in Waves," in *ASME 2014 33rd International Conference on Ocean, Offshore and Arctic Engineering*, 2014, pp. V09BT09A038–V09BT09A038.

[2] "Rhinoceros." [Online]. Available: http://www.rhino3d.com/.

[3] W.E. Cummins, "The Impulse Response Function and Ship Motions," David Taylor Model Dasin-DTNSRDC, 1962.

[4] C.H. Lee and J.N. Newman, "WAMIT® User Manual." WAMIT, Inc.

[5] "Nemoh Website." [Online]. Available: http://lheea.ec-nantes.fr/doku.php/emo/nemoh/.

[6] M. Lawson, Y.-H. Yu, A. Nelessen, K. Ruehl, and C. Michelen, "Implementing Nonlinear Buoyancy and Excitation Forces in the WEC-Sim Wave Energy Converter Modeling Tool," in *Proceedings of the 33rd International Conference on Ocean, Offshore and Arctic Engineering (OMAE 2014)*, San Francisco, CA, 2014.

[7] K. Ruehl, "Preliminary Verification and Validation of WEC-SIM, an Open Source Wave Energy Converter Design Tool," in *Proceedings of the ASME 2014 33rd International Conference on Ocean, Offshore and Arctic Engineering*, 2014.

[8] "Competition on Hydrodynamic Modelling of a Rigid Body." [Online]. Available: http://www.eeng.nuim.ie/coer/view_event.php?id=EV008. [Accessed: 14-Dec-2014].

[9] "FAST v8 (NWTC Information Portal)." [Online]. Available: https://nwtc.nrel.gov/FAST8.

[10] J.M. Jonkman, A.N. Robertson, and G.J. Hayman, "HydroDyn User Guide."